

Evaluating Various Components of Total Radiance Measured by Ocean Color Satellite Sensors in Oceanic and Coastal Regions

Kimberly Tejada^{1,2}, Soe Hlaing^{2,3}, and Alex Gilerson^{2,3}
¹Massachusetts High School 2, ²NOAA CREST, ³The City College of New York

ABSTRACT

With rising air pollution and harmful algal blooms in coastal regions, large-scale monitoring of these areas is necessary towards analyzing environmental changes by natural causes and anthropogenic impacts. The most economical way to carry out monitoring of coastal and oceanic areas is through satellite sensors designed for ocean color (OC) remote sensing. These sensors have been successfully applied for measuring and quantifying the various atmosphere and oceanic conditions around the globe. Notably, OC satellite sensors are employed to measure the reflected light radiance field, quantified as radiation energy per unit solid angle per unit area (usually in mW/cm²/μm/sr). The total top of atmosphere (TOA) radiance light field measured by the OC satellite sensor (L_T) is composed of various parts: aerosol radiance (L_a), molecule radiance (L_m), radiance reflected from sea surface (L_s), and water-leaving radiance (L_w). Using the Near Infrared (NIR) algorithm by Gordon (1994), radiance data can be used to assess information on the constituents of atmosphere and sea water. However, there is a significant need to improve this retrieval algorithm for coastal regions and to gain further information for ascertaining atmospheric and sea water constituents through the radiance contributions of each component to satellite-measured L_T. Therefore, the purpose of this project was to evaluate and quantify the contributions of various radiance components to satellite-measured TOA L_T for both oceanic and coastal

INTRODUCTION

The ocean possesses vital roles on earth, contributing to climate and weather, human industry, and so forth. Statistically, the ocean covers over 2/3 of the Earth's surface. Regarding human relevance, over 3 billion people rely on marine areas for their livelihood, with a market value of \$3 trillion per year for ocean-related resources and industries. Essentially, it is necessary to monitor oceanic and coastal regions.

Remote sensing through ocean color (OC) imagery is one of the major and efficient methods towards monitoring the ocean. OC imagery can detect and identify types of algal biomass and other contributing ocean pigments, and determine mineral concentrations. Although current satellite OC remote sensing algorithms for analyzing oceanic waters

KNOWLEDGE BASE



Fig. 1: Satellite image of Long Island.
(Photo from USDA Farm Service Agency)

❖ As sunlight travels through the atmosphere and the water, light is scattered and absorbed based on optical properties of the contents in air and water

❖ This light carries spectral information about the particular composition of the area, making it ideal for passive remote sensing

❖ **Radiance**-measure of radiation or electromagnetic energy per unit solid angle (mW/cm²/μm/sr)

$$\tau_r(\lambda, P_0 + \Delta P) = \tau_r(\lambda, P_0) \frac{P_0 + \Delta P}{P_0}$$

$$L_T[\tau_r(\lambda, P_0 + \Delta P)] = L_T[\tau_r(\lambda, P_0)] \frac{1 - \exp[-\tau_r(\lambda, P_0 + \Delta P)/\cos\theta]}{1 - \exp[-\tau_r(\lambda, P_0)/\cos\theta]}$$

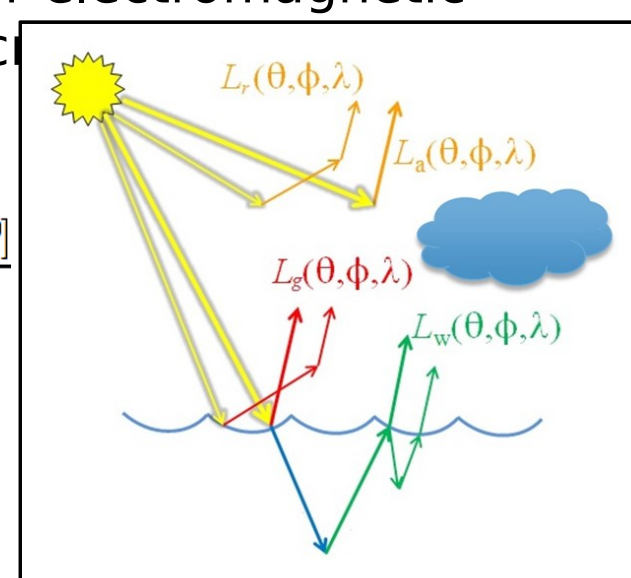


Fig. 2: Process of sunlight traveling to ocean.
(Image from Ocean Optics Web Book)

$L_T = L_a + L_r + t^*L_w + L_g$
 L_T -> Total top of atmosphere radiance
 L_a -> Aerosol radiance
 L_m -> Molecule radiance
 t*L_w -> Water-leaving radiance
 L_g -> Surface-water/glint radiance

❖ NIR algorithms usually used to determine the radiances for oceanic waters where atmospheric contribution is relatively low.

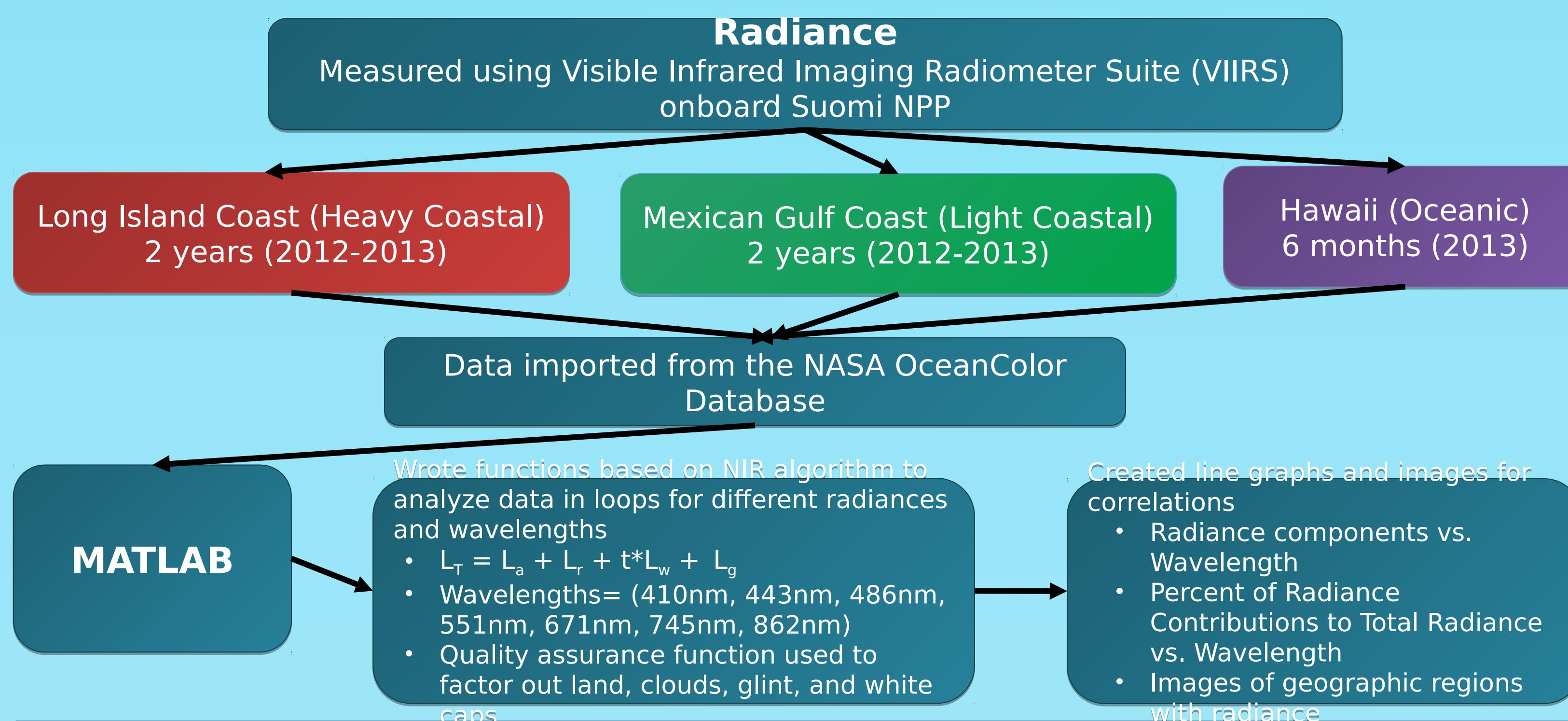
❖ Water-leaving radiance in oceanic regions approximately 10% on spectral average.

❖ Identify necessary corrections to improve the NIR algorithm of coastal waters.

❖ Evaluate the relationship between component radiances and wavelength.

❖ Quantify the contributions of component radiances out of total radiance.

Coastal Regions



DATA ANALYSIS

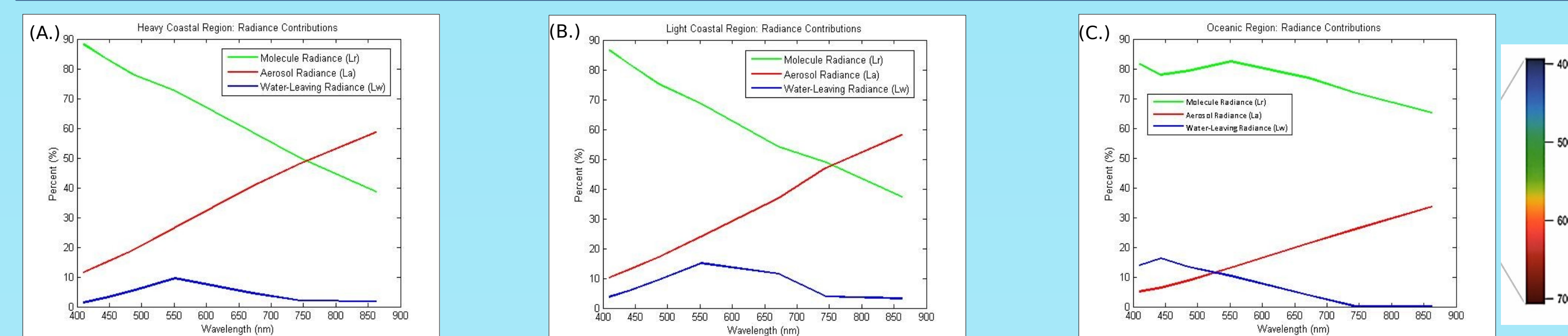


Fig. 3: Graphs of the mean radiance contribution to the total top of atmosphere radiance (L_T) by wavelength. (A.) Graph 3A is for the heavy coastal area. The water-leaving radiance (L_w) is greatest at 550 nm with around a 10% contribution. (B.) Graph 3B illustrates the light coastal region. L_w is also highest at 550 nm with a contribution of approximately 16%. (C.) Graph 3C demonstrates the oceanic region. L_w is greatest at 443nm with an 18% contribution; however, it has only 10% contribution at 550 nm.

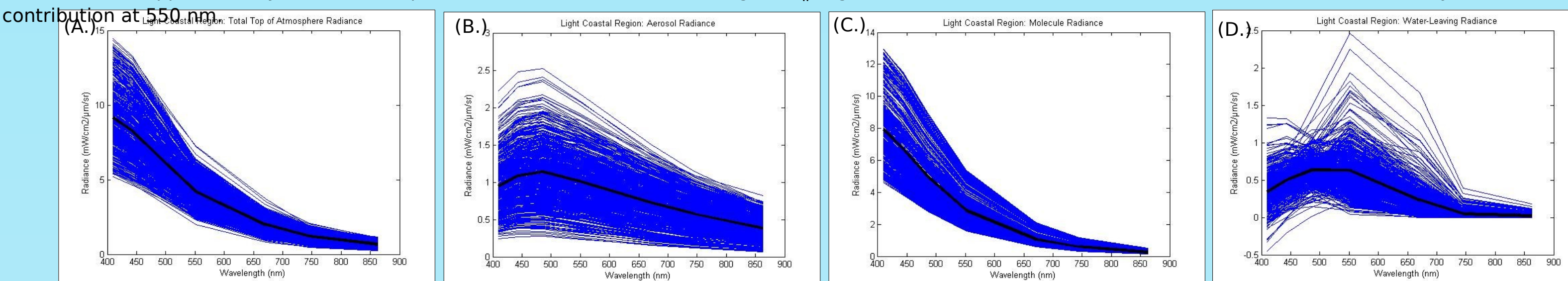


Fig. 4: Graphs of the different radiances versus wavelength in the light coastal region. All four radiances exhibit an indirect relationship. (A.) L_T has a maximum of 9 (mW/cm²/μm/sr) at 412nm with a minimum of 1 (mW/cm²/μm/sr) at 862nm. (B.) Aerosol radiance (L_a) has a maximum of 1.2 (mW/cm²/μm/sr) at 490 nm and a minimum of 0.5 (mW/cm²/μm/sr) at 862 nm. (C.) Molecule radiance (L_m) has a maximum of 8 (mW/cm²/μm/sr) at 412nm and a minimum of 0.1 (mW/cm²/μm/sr) at 862 nm. (D.) L_w has a maximum of 0.5 (mW/cm²/μm/sr) at 450 nm and a minimum of 0 (mW/cm²/μm/sr) at 862 nm.

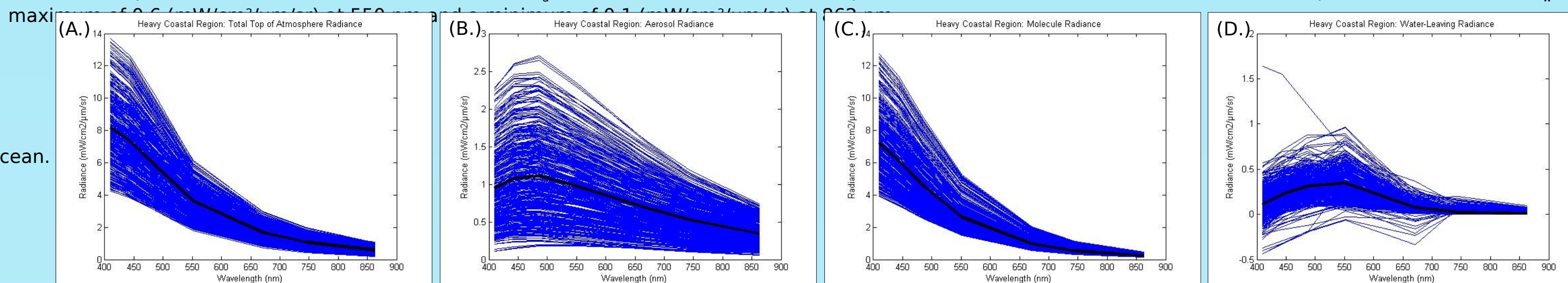


Fig. 5: Graphs of the different radiances versus wavelength in the heavy coastal region. All four radiances exhibit an indirect relationship. (A.) L_T has a maximum of 8 (mW/cm²/μm/sr) at 412nm with a minimum of 0.25 (mW/cm²/μm/sr) at 862nm. (B.) Aerosol radiance (L_a) has a maximum of 1.2 (mW/cm²/μm/sr) at 490 nm and a minimum of 0.3 (mW/cm²/μm/sr) at 862 nm. (C.) Molecule radiance (L_m) has a maximum of 7 (mW/cm²/μm/sr) at 412nm and a minimum of 0.1 (mW/cm²/μm/sr) at 862 nm. (D.) L_w has a maximum of 0.5 (mW/cm²/μm/sr) at 450 nm and a minimum of 0 (mW/cm²/μm/sr) at 862 nm.

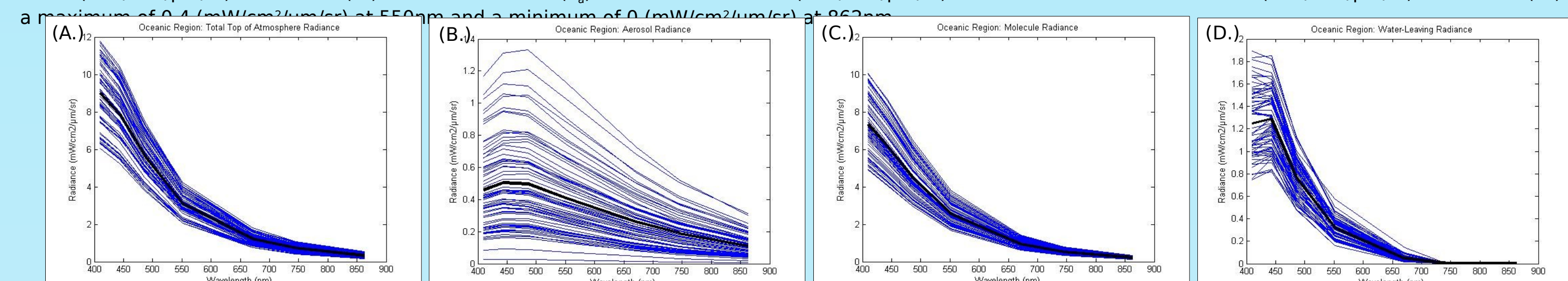


Fig. 6: Graphs of the different radiances versus wavelength in the oceanic region. All four radiances exhibit an indirect relationship. (A.) L_T has a maximum of 9 (mW/cm²/μm/sr) at 400 nm with a minimum of 1 (mW/cm²/μm/sr) at 862nm. (B.) Aerosol radiance (L_a) has a maximum of 0.5 (mW/cm²/μm/sr) at 490 nm and a minimum of 0.1 (mW/cm²/μm/sr) at 862nm. (C.) Molecule radiance (L_m) has a maximum of 0.5 (mW/cm²/μm/sr) at 412nm and a minimum of 0.1 (mW/cm²/μm/sr) at 862nm. (D.) L_w has a maximum of 1.3 (mW/cm²/μm/sr) at 450 nm and a minimum of 0 (mW/cm²/μm/sr) at 862 nm.

DATA ANALYSIS (Continued)

Examples of VIIRS Images used in

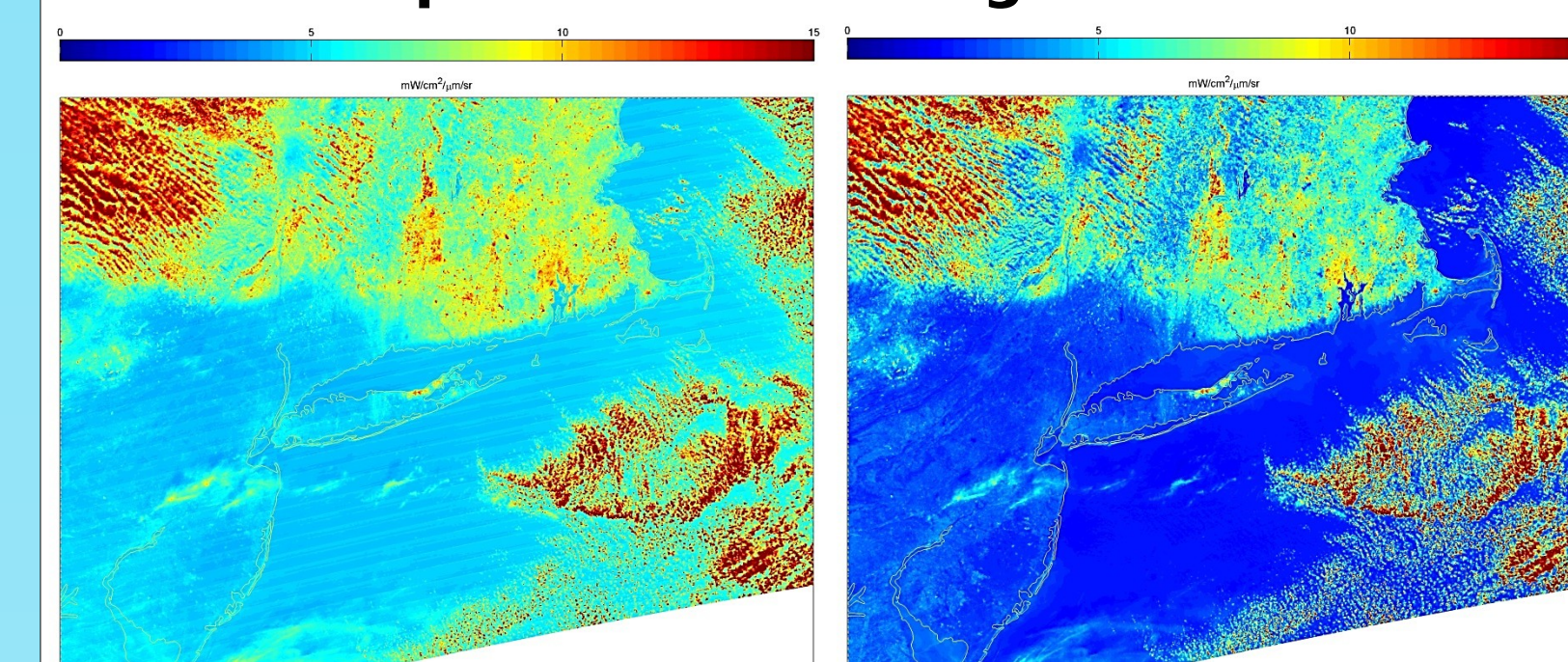


Fig. 7: VIIRS images of Long Island region at 412 and 550 nm channels obtained on January 20th 17:41 GMT through the Suomi NPP through passive remote sensing.

DISCUSSION

❖ **Purpose:** To evaluate the contributions from different components of radiances to the total top of atmosphere radiance for the improvement of atmospheric correction algorithm for the OC remote sensing especially for coastal regions.

❖ Results for the radiance data reveal the oceanic region had the greatest water-leaving radiance (L_w) contribution in the blue part of the spectrum; coastal regions had the higher aerosol radiance (L_a). Also, some coastal L_w data retrievals are negative (which are subsequently excluded from the analysis); in contrast oceanic L_w data had no negative retrievals.

❖ For both heavy and light coastal regions, their radiance contributions reveal that L_w composes less than 10% of the total top of atmosphere radiance (L_T). Notably, L_w had its greatest contribution for 550 nm (green light). From 750 nm to 862 nm (red end), L_w contribution approaches 0. L_a exceeds molecule radiance (L_m) at 750 nm and higher (red). Also, L_w at the near infrared (750 to 862 nm) was not 0, and L_a contribution at those wavelengths were around 60%.

❖ For the oceanic region, its radiance contribution shows a L_w up to 18%. In contrast to the coastal results, L_w contribution is greatest at 450 nm (blue light). From 750 nm and greater (red), the L_w contribution is 0. Distinctly, L_w contribution is greater than L_a from 400 to 525 nm (purple, blue and green).

❖ Limitations to this study may have been the difference in the time span for data collection between the coastal and oceanic regions and calibration issues with the sensor.

❖ Coastal regions were more sensitive and error prone than oceanic areas due to their smaller L_w contribution. Additionally, L_w radiance contributions in coastal areas were always lower than the aerosol and molecular contribution.

❖ Research findings underscored the limitations of the current atmospheric correction algorithm which assumed that L_w at the near infrared (750 to 862 nm) was 0, in which coastal L_w was not 0.

❖ Difficulties with accurate OC remote sensing of the coastal regions, such as negative L_w radiance retrievals,

REFERENCES & ACKNOWLEDGEMENTS

Feldman, Gene Carl. "OceanColor Documents." NASA OceanColor Database. NASA, 7 Dec. 2011. Web. <http://oceancolor.gsfc.nasa.gov/DOCS/MSL12/MSI12_prod.html>.
 Gordon, Howard R., and Menghua Wang. Retrieval of Water-leaving Radiance and Aerosol Optical Thickness over the Oceans with SeaWiFS: A Preliminary Algorithm. Applied Optics. Optical Society of America, 20 Jan. 1994. Web.
 Hlaing, Soe, Tristan Harmel, Alex Gilerson, Robert Foster, Alan Weidemann, Robert Amone, Menghua Wang, and Samir Ahmed. Evaluation of the VIIRS Ocean Color Monitoring Performance in Coastal Regions. Remote Sensing of Environment. ELSEVIER, 17 Aug. 2013. Web.
 Mobley, Curtis. "Remote Sensing: The Atmospheric Correction Problem." Ocean Optics Web Book. Ocean Optics Web Book, 5 Oct. 2011. Web. 1 Aug. 2014. <http://www.oceanopticsbook.info/view/remote_sensing/the_atmospheric_correction_problem>.
 Wang, Menghua. A Refinement for the Rayleigh Radiance Computation with Variation of the Atmospheric International Journal of Remote Sensing. Taylor & Francis, 20 Dec. 2005. Web.
 This research project was funded by the National Oceanic and Atmospheric Administration-Cooperative Remote Sensing Science and Technology Center (NOAA-CREST, NA11REG4910004) and supported by the Pinkerton Foundation.